

# Optical properties of Teflon<sup>®</sup> AF amorphous fluoropolymers

Min K. Yang

Roger H. French

DuPont Co. Central Research

Experimental Station

Wilmington, Delaware 19880-0400

E-mail: min.k.yang@usa.dupont.com

Edward W. Tokarsky

DuPont Fluoropolymer Solutions

Chestnut Run Plaza

Wilmington, Delaware 19880-0713

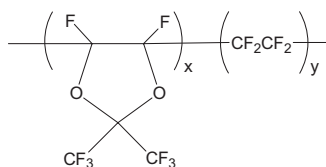
**Abstract.** The optical properties of three grades of Teflon<sup>®</sup> AF—AF1300, AF1601, and AF2400—were investigated using a J.A. Woollam VUV-VASE spectroscopic ellipsometry system. The refractive indices for each grade were obtained from multiple measurements with different film thicknesses on Si substrates. The absorbances of Teflon<sup>®</sup> AF films were determined by measuring the transmission intensity of Teflon<sup>®</sup> AF films on CaF<sub>2</sub> substrates. In addition to the refractive index and absorbance per cm (base 10), the extinction coefficient ( $k$ ), and absorption coefficient ( $\alpha$ ) per cm (base e), Urbach parameters of absorption edge position and edge width, and two-pole Sellmeier parameters were determined for the three grades of Teflon<sup>®</sup> AF. We found that the optical properties of the three grades of Teflon<sup>®</sup> AF varied systematically with the AF TFE/PDD composition. The indices of refraction, extinction coefficient ( $k$ ), absorption coefficient ( $\alpha$ ), and absorbance ( $A$ ) increased, as did the TFE content, while the PDD content decreased. In addition, the Urbach edge position moved to a longer wavelength, and the Urbach edge width became wider. © 2008 Society of Photo-Optical Instrumentation Engineers. [DOI: 10.1117/1.2965541]

Subject terms: fluoropolymer; absorbance absorption coefficient; VUV ellipsometry.

Paper 07086R received Oct. 24, 2007; revised manuscript received May 16, 2008; accepted for publication Jun. 6, 2008; published online Aug. 13, 2008.

## 1 Introduction

Teflon<sup>®</sup> AF fluoropolymers are widely used in industrial and commercial applications. Teflon<sup>®</sup> AF [chemical name: fluorinated (ethylenic-cyclo oxaliphatic substituted ethylenic) copolymer] is a family of amorphous fluoropolymers based on copolymers of 2,2-bis(trifluoromethyl)-4,5-difluoro-1,3-dioxole (PDD).<sup>1</sup> Its chemical structure is shown here:<sup>2,3</sup>



The PDD dioxole monomer in Teflon<sup>®</sup> AF yields polymers that have unexpected properties. Teflon<sup>®</sup> AF is a copolymer of PDD and tetrafluoroethylene (TFE). The principle difference in three grades of Teflon<sup>®</sup> AF polymers (AF1300, AF1601, and AF2400) is based solely on the relative amount of the dioxole monomer (TFE:PDD) in the basic polymer chain (Table 1). In addition to outstanding chemical, thermal, and surface properties, Teflon<sup>®</sup> AF fluoropolymers have unique electrical, optical, and solubility characteristics.

The Teflon<sup>®</sup> AF fluoropolymers are distinct from other fluoropolymers in that they are soluble in selected solvents and have high gas permeability, high compressibility, high creep resistance, and low thermal conductivity. Teflon<sup>®</sup> AF

fluoropolymers have the lowest dielectric constant of any known solid polymer, and this makes them attractive for demanding electronics applications. Teflon<sup>®</sup> AF polymers have the lowest index of refraction of any known polymer, making them very suitable as low-index claddings for waveguide applications. Because of the combination of electric and optical properties, the use of Teflon<sup>®</sup> AF fluoropolymers is very attractive in photonics and photovoltaics. Teflon<sup>®</sup> AF is the first polymer to demonstrate a transparency possibility of at least 40% of incident light at 157 nm making it to the bottom of the resist layer for purposes of sharp pattern development.<sup>4</sup>

This paper describes the optical properties such as refractive index, extinction coefficient ( $k$ ), absorbance, absorption coefficient ( $\alpha$ ), and absorption edge that we have extensively studied. We have determined these optical properties and found the relationship between those prop-

**Table 1** Physical properties of Teflon<sup>®</sup> AF grades 1300, 1601, and 2400.

| TAF Grade | Specific Gravity<br>ASTM D792 | TFE/PDD<br>Composition Ratio<br>(mol %) | $M_n$ , Nominal |
|-----------|-------------------------------|---|-----------------|
| AF1300    | 1.88                          | 50/50                                   |                 |
| AF1601    | 1.78                          | 35/65                                   | 225 M           |
| AF2400    | 1.67                          | 11/89                                   | 600 M           |

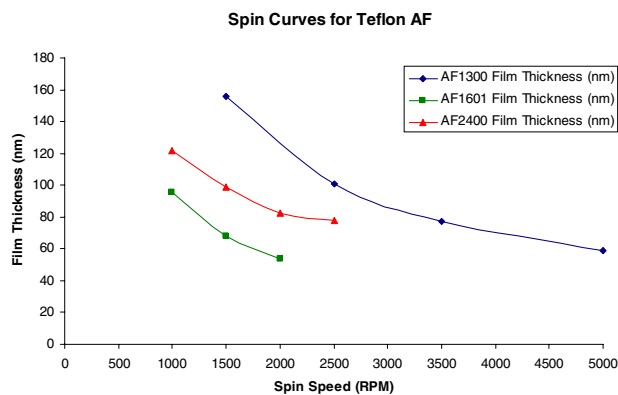


**Fig. 1** Experimentally determined spin curves for Teflon® AF grades 1300, 1601, and 2400, spun on silicon wafers vapor-primed with HMDS.

erties for three grades of Teflon® AF fluoropolymers.

## 2 Experimental and Analytical Techniques

### 2.1 Sample Preparation

For VUV spectroscopic ellipsometry, a spin coating method was used for obtaining thin uniform coatings on silicon wafers. A Brewer Science spincoater/hotplate (Brewer Science, Rolla, Missouri) was used to spin Teflon® AF solution onto hexamethyldisilazane (HMDS) vapor-primed silicon wafers. In order to obtain various thicknesses of film, the spinning speed range was set to 1000 RPM, 1500 RPM, 2000 RPM, 2500 RPM, 3500 RPM, and 5000 RPM, respectively, for 60 s. Different thicknesses of film improves confidence in the results, as light travels different paths through the film. The bake temperature was 140° for 60 s. In order to obtain a workable spinning solution, samples of 6.5 wt% Teflon® AF1300 and AF1601 were diluted by adding FC-40 surfactant (Fluorinert electronic liquid manufactured by 3M) to the Teflon® AF spinning solution. The solids ratio of FC-40 to Teflon® AF polymer for AF1300 is 1 to 0.022 and for AF1601 is 1 to 0.020. Various film thicknesses between 60 and 160 nm were obtained by use of a rotation speed range of 1500 to 5000 RPM and a spinning time of 60 s for AF1300. Various film thicknesses between 50 and 100 nm were obtained by use of a rotation speed range of 1000 to 2000 RPM and a spinning time of 60 s for AF1601. A sample Teflon® AF 400S1-100-1 (Teflon® AF2400) was diluted by adding FC-40 surfactant to the AF2400 for a workable solution. The solids ratio of FC-40 to Teflon® AF polymer for AF2400 is 1 to 0.008. Various film thicknesses between 70 and 120 nm were obtained by use of a rotation speed range of 1000 to 2500 RPM and a spinning time of 60 s. Figure 1 shows the experimentally determined spin curves for these solutions of Teflon® AF grades 1300, 1601, and 2400, determined on HMDS-vapor-primed silicon wafers.

For transmission samples, droplets of undiluted original Teflon® AF1300 and AF1601 solutions were dispensed on the 13 × 1 mm bare CaF<sub>2</sub> substrate (Corning, Brookfield, Massachusetts) and slowly dried in a closed metal sample box for several days in order to obtain a crack-free thick film. For improved wetting for the undiluted original Teflon® AF2400 solution, it was deposited on 13 × 1 mm

CaF<sub>2</sub> substrates that were also vapor primed with HMDS and dried under the same conditions as the other two grades. Film thicknesses were measured using a stylus profilometer, Dektak 3ST (Veeco, Woodbury, NY).

### 2.2 Spectroscopic Ellipsometry and Analysis

The variable-angle spectroscopic ellipsometry (VASE) measurements were performed with the VUV-VASE VU-302 instrument (J.A. Woollam Co., Lincoln, Nebraska), which has a range from 0.69 to 8.55 eV (1800 to 145 nm) and employs MgF<sub>2</sub> polarizers and analyzers rather than the more common calcite optics. The spectrometer was upgraded from single beam to dual beam for more accurate transmission measurements and better instrument stability. The instrument has an MgF<sub>2</sub> auto-retarder and is fully nitrogen purged to avoid absorption of VUV light by ambient oxygen and water vapor, which is important at wavelengths below 200 nm. Light from both the deuterium lamp and the xenon lamp passes through a double-chamber Czerny-Turner-type monochromator to provide wavelength selection and stray-light rejection. The spot diameter of the light source on the surface of the sample is 2 mm. Computer-controlled slit widths can adjust the bandwidth to insure adequate spectral resolution of optical features in the data such as the closely spaced interference oscillations, which arise in very thick film. A photomultiplier tube is utilized for signal detection in the ultraviolet. A stacked Si/InGaAs photodiode detector is used for longer wavelengths. Ellipsometric measurements were conducted using light incident at angles of 55 deg to 80 deg relative to normal on the front surface of the sample, the back of which was roughened with coarse polishing paper. The instrument measures the ellipsometric parameters  $\Psi$  and  $\Delta$ , which are defined<sup>5</sup> by Eq. (1):

$$\tan(\Psi)e^{i\Delta} = \left| \frac{R_p}{R_s} \right|, \quad (1)$$

where  $R_p/R_s$  is the complex ratio of the  $p$ - and  $s$ -polarized components of the reflected amplitudes. These parameters are analyzed using the Fresnel equations<sup>6,7</sup> in a computer-based modeling technique, including a surface roughness layer to directly determine the optical constants.<sup>8,9</sup> VUV-VASE VU-302 measurements for this experiment were taken from wavelength range 145 nm to 1550 nm and at multiple angles (55 deg to 0 deg). Variable angles improve confidence, as light travels different paths through the film.

The ellipsometry data, taken from the film on silicon substrate, was fit to determine the polymer film thickness, roughness, thickness nonuniformity, and complex refractive index<sup>10</sup> (Fig. 2). Initially a parameterized model was used to describe the Teflon® AF film optical constants over the wide spectral range.

The Teflon® AF films were modeled using tabulated optical constants from Woollam for silicon and SiO<sub>2</sub>. A thin surface layer was described in the optical model using roughness, which is an effective medium approximation (EMA) consisting of 50/50 mix of organic film and void ( $n=1$ ). In the initial stage, a Cauchy dispersion model was used to fit the transparent region of 450 nm to 1550 nm. The final model was determined by fitting the optical constants on a point-by-point basis over the full spectral range

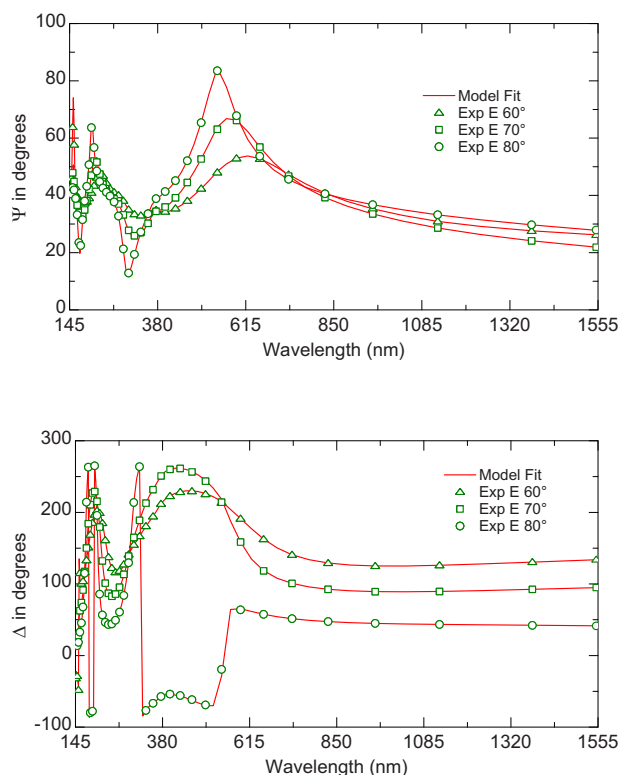


**Fig. 2** Ellipsometric data  $\Psi$  and  $\Delta$  measured on a Teflon<sup>®</sup> AF1300 grade thin film on a silicon wafer and the model fit results.

in which the data in each single wavelength are fit separately. A typical application for this data class was chosen as displaying wavelength-by-wavelength fit parameter confidence limits for optical constants. This method does not insist on Kramers-Kronig consistency.

Teflon<sup>®</sup> AF1300 is used as an example of the ellipsometric analysis. The ellipsometry data (Fig. 2), taken from the film on silicon substrate, was fit, in a linear regression sense, to a thin-film optical model<sup>11</sup> to determine its film thickness roughness and thickness nonuniformity, and complex refractive index [Eq. (2)].<sup>12</sup>

$$\hat{n} = n + ik. \quad (2)$$

### 2.3 Sellmeier Equations

Sellmeier equations and their fitted parameters have been employed for many years as a convenient way to permit the calculation of the index of refraction of transparent materials at arbitrary wavelengths. We have evaluated two 2-pole

(1 UV and 1 IR) [Eq. (3) and Eq. (4)] and one 3-pole (2 UV and 1 IR) [Eq. (5)] Sellmeier equations fitted to the three grades of Teflon<sup>®</sup> AF to parameterize the wavelength dispersion of the index of refraction:

$$n^2(\lambda) = 1 + \frac{B_1\lambda^2}{\lambda^2 - C_1} + \frac{B_2\lambda^2}{\lambda^2 - C_2}, \quad (3)$$

$$n^2(\lambda) = A + \frac{B_1\lambda^2}{\lambda^2 - C_1} + \frac{B_2\lambda^2}{\lambda^2 - C_2}, \quad (4)$$

$$n^2(\lambda) = 1 + \frac{B_1\lambda^2}{\lambda^2 - C_1} + \frac{B_2\lambda^2}{\lambda^2 - C_2} + \frac{B_3\lambda^2}{\lambda^2 - C_3}, \quad (5)$$

where  $\lambda$  is wavelength,  $n^2(\lambda)$  is the square of the refractive index, the coefficient  $A$  is an approximation of the short-wavelength (UV) absorption contributions to the refractive index at longer wavelengths, and  $B_{1,2,3}$  and  $C_{1,2,3}$  are the parametrically fitted Sellmeier coefficients associated with a given optical material. This equation was deduced in 1871 by Sellmeier and was developed by Cauchy as Cauchy's equation for modeling dispersion.<sup>13</sup> The Sellmeier equation is usually valid only in high-transparency spectral regions. We find that the two-pole Sellmeier equation given in Eq. (4) gives the minimum standard error of the fit for these samples, and these Sellmeier parameters are summarized in Table 2.

### 2.4 Optical Transmission and Absorption Coefficient

The optical absorbance of the Teflon<sup>®</sup> AF film was determined by measuring the transmission intensity of CaF<sub>2</sub> substrates and films of different thicknesses on CaF<sub>2</sub> substrates. Once the transmission spectra of the substrate and the film coated on that substrate were determined, the film optical absorbance per cm (base 10) was then determined by Eq. (6):

$$A/\text{cm} = \frac{\log_{10}(T_{\text{substrate}}/T_{\text{film}})}{t_{\text{film}}}, \quad (6)$$

where  $T$  is the transmission,  $t$  is the thickness of film, and  $A/\text{cm}$  is the absorbance per centimeter (base 10). Using multiple samples of different film thickness, one can then solve the resulting system of equations and determine the reproducibility and a standard deviation of the optical absorbance per centimeter.

Transmission-based measurements also require that the film thickness of the sample on the substrate be optimized

**Table 2** Two-pole Sellmeier parameters.

| TAF Grade | $A$   | $B_1$ | $C_1$ | $B_2$ | $C_2$  |
|-----------|-------|-------|-------|-------|--------|
| AF1300    | 1.517 | 0.184 | 0.016 | 1     | 104.66 |
| AF1601    | 1.461 | 0.226 | 0.014 | 1     | 119.03 |
| AF2400    | 1.456 | 0.181 | 0.014 | 1     | 159.28 |

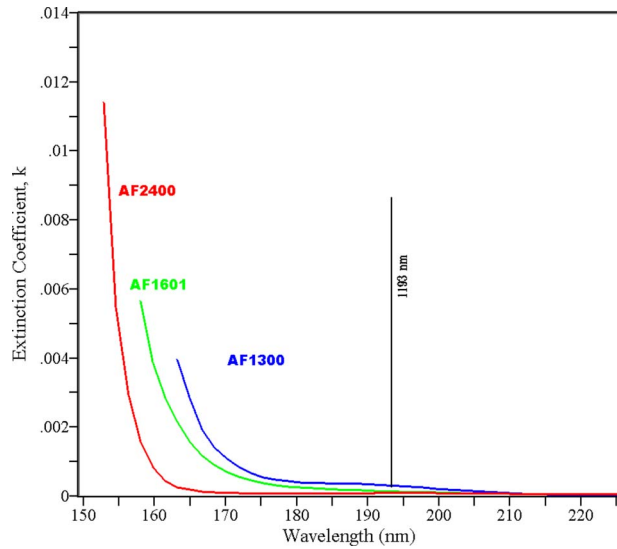


**Fig. 3** Extinction coefficient  $k$  determined from transmission measurement for three grades of Teflon® AF.

for the dynamic range of the technique so that the transmittance of the film and substrate falls in the range from 3 to 90%. If the transmittance falls much below 1%, the accuracy of the measurement is severely degraded and erroneous results appear.<sup>14</sup> Much of the uncertainty comes from the antireflective effect of thin polymer film when coated on CaF<sub>2</sub>. That is, the small amount of light absorbed by a highly transparent film is lost in comparison to the transmission increase resulting from decreased reflectivity from the antireflective effect. In the worst such case,  $T_{\text{sample}}$  is greater than  $T_{\text{substrate}}$ , and the calculated absorbance goes negative.<sup>15</sup>

As in all experimental measurements, the accuracy of the measured values is a function of the sample and measurement apparatus. The inherent sensitivity of spectral transmission and absorbance measurements is affected by the optical path length of the sample and the transmission drop that occurs as light transmits through the sample in the measurement. As the transmission drop decreases, the accuracy of the absorbance measurement decreases. A transmission difference of  $\sim 0.1\%$  is near the limit of the measurement method.

Once the extinction coefficient  $k$  (from ellipsometry, Fig. 3) and the base-10 absorption coefficient  $A$  (Fig. 4) have been determined, the base-e optical absorption parameter  $\alpha$  (Fig. 5) can be determined using Eq. (7). The absorption coefficient,  $\alpha$ , corresponds to the attenuation of the light transmitted through the sample and is calculated on a natural logarithm basis. Since the absorbance per cm,  $A$ , is determined from the base-10 logarithm of the optical density given in Eq. (6), a value of  $\ln(10)$ , or 2.302585, is introduced into Eq. (6) and Eq. (7). Both  $k$  and  $\alpha$  are inherent optical properties of the material. On the other hand, absorbance/cm is frequently based only on transmission measurements and thus neglects effects arising from the index mismatch between the film and substrate, thin film interference effects, and film nonuniformity effects.

The fundamental absorption edge spectra have been determined<sup>16</sup> by Eq. (7):

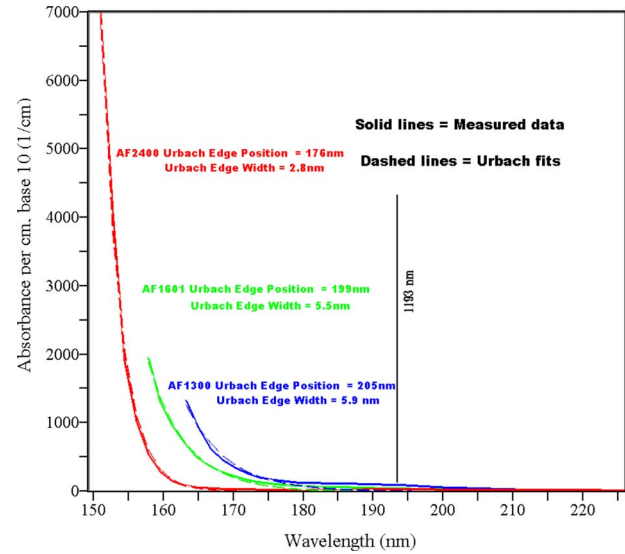


**Fig. 4** Optical absorption edge (absorbance fits) of three grades of Teflon® AF with their corresponding Urbach edge fits (dashed lines).

$$\alpha = 4\pi k/\lambda, \quad (7)$$

where  $\alpha$  is the optical absorption coefficient (base e),  $\lambda$  is the wavelength of the light source, and  $k$  is the extinction coefficient. The relationship between the base-e absorption coefficient  $\alpha$  and the base-10 absorption coefficient  $A$  is given in Eq. (8):

$$A = \frac{\log_{10}(T_1) - \log_{10}(T_2)}{t} = \frac{1}{\ln(10)} \frac{\ln(T_1) - \ln(T_2)}{t} \\ = \frac{1}{\ln(10)} \alpha, \quad (8)$$

where  $T_1$  is the transmission of the substrate,  $T_2$  is the transmission of the film, and  $t$  is the thickness of the film.

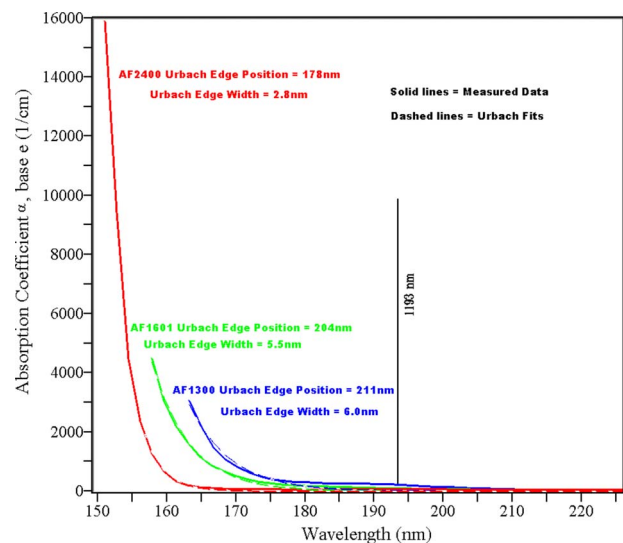


**Fig. 5** Optical absorption edge (absorbance coefficient fits) of three grades of Teflon® AF with their corresponding Urbach edge fits (dashed lines).

## 2.5 Urbach Analysis of Absorption Edges

Urbach edge analysis is a useful way to parametrically characterize a film's optical absorption edge and to potentially distinguish intrinsic and extrinsic contributions to the absorbance.<sup>17</sup> Urbach<sup>18</sup> originally observed that a material's optical absorption for energies below the fundamental optical absorption edge is exponential in nature and can be characterized by the Urbach edge energy ( $E_0$ ) and the Urbach width ( $W$ ), which is related to the slope of the Urbach edge [using the nm↔eV conversion  $\lambda(\text{nm})=1239.8/E$  (eV)].

### 2.5.1 Urbach analysis of the absorption coefficient ( $\alpha$ ) and the absorbance ( $A$ )

When Urbach fits an exponential to  $\alpha$ , the equations used are:

$$\alpha(E) = H_\alpha \exp\left(\frac{E - E_{0\alpha}}{W_\alpha}\right), \quad (9)$$

$$\ln(\alpha) = \frac{E - (E_{0\alpha} - h_\alpha W_\alpha)}{W_\alpha}, \quad (10)$$

where the absorption coefficient  $\alpha$  as a function  $E$  is characterized by the Urbach edge energy ( $E_0$ ) and the Urbach width ( $W$ ). The intercept  $E_{0\alpha}$  (energy at which  $\alpha=1$ ) is the quantity of interest. When Urbach fits an exponential to  $A$ , the equations used are:

$$A(E) = H_A \exp\left(\frac{E - E_{0A}}{W_A}\right), \quad (11)$$

$$\ln(A) = \frac{E - (E_{0A} - h_A W_A)}{W_A}. \quad (12)$$

The intercept  $E_{0A}$  (energy at which  $A=1$ ) is the quantity of interest. The relationship between  $E_{0\alpha}$  and  $E_{0A}$  is obtained as follows:

$$A(E) = H_A \exp\left(\frac{E - E_{0A}}{W_A}\right) = \frac{\alpha}{\ln(10)} = \frac{H_\alpha}{\ln(10)} \exp\left(\frac{E - E_{0\alpha}}{W_\alpha}\right). \quad (13)$$

### 2.5.2 Relationships between slopes and intercepts for Urbach fits to $A$ versus $\alpha$

Note that Urbach actually fits the exponential equations shown earlier. This is done because the error statistics are known in data space ( $A$  and  $\alpha$ ), not in  $\ln(\text{data})$  space. The equations given here are the easiest to use to understand the slope and intercepts that are provided in the solution.

The preceding exponential equations that are used by Urbach for fitting can be transformed to a linear form by taking the logarithm of the data. When we do this, we obtain the following: straight line equations, with slopes  $m$  and intercepts  $b$ .

$$\ln(\alpha) = m_\alpha * E + b_\alpha, \quad (14)$$

$$\ln(A) = m_A * E + b_A. \quad (15)$$

The intercept energies  $-b_\alpha$  [energy at which  $\ln(\alpha)=1$ ], and  $-b_A$  [energy at which  $\ln(A)=1$ ] are the quantities of interest.

Using the conversion between  $\alpha$  and  $A$ , we can find the relationship between the slopes and intercepts for  $A$  versus  $\alpha$ . What one finds is that the computed Urbach edge widths will be the same for fits to  $A$  or  $\alpha$ :

$$W_\alpha = W_A. \quad (16)$$

The intercept energies  $E_{0A}$  and  $E_{0\alpha}$ , as reported by Urbach, are related by:

$$E_{0\alpha} = E_{0A} + \ln(2.302585)/m_A, \quad (17)$$

$$E_{0\alpha} = E_{0A} + \ln(2.302585) * W_A. \quad (18)$$

## 3 Results

### 3.1 Complex Index of Refraction ( $n+ik$ )

The refractive index ( $n$  and  $k$ ), film thickness of Teflon® AF films, and transmission intensity of Teflon® AF films were determined over the wavelength range 145 nm to 1550 nm.

In order to obtain the best quality of uniform and crack-free thin films by spin coating, Teflon® AF films with thicknesses in the range of 50 to 160 nm were measured instead of the 200-nm-thick films commonly studied in ellipsometry. Therefore, these samples are a good candidate for multiple sample analysis performed by simultaneously fitting the data from two or more samples. This is a very powerful method for determining optical constants because fit parameters are coupled between the models to take advantage of the additional information provided by the use of multiple samples. A good multiple sample analysis is effective only if all films have the same optical constants.

The complex indices of refraction for the three grades of Teflon® AF, AF1300, AF1601, and AF2400 are shown in Fig. 6 and Table 3. A plot of the extinction coefficient ( $k$ ) determined from transmission measurement of the film on the CaF<sub>2</sub> substrates is shown in Fig. 3.

The results of the indices of refraction calculated from the Sellmeier equations are quite similar to those determined from the Cauchy model. The index of refraction versus wavelength data can be provided by the Sellmeier equation without the need for extensive tables.

### 3.2 Transmission and Absorption Coefficient

For the determination of the optical absorption of the film micron-thick films were measured. These thicker films are more susceptible to the effects of nonuniformity and finite spectrometer bandwidth. Ellipsometers that include a retarding element are capable of measuring percent depolarization.<sup>10</sup> Both film nonuniformity and finite-bandwidth can depolarize the measurement beam. We quantify these nonideal effects and model their behavior during analysis of experimental data. In this manner, the optical constants can be determined with a higher degree of certainty.

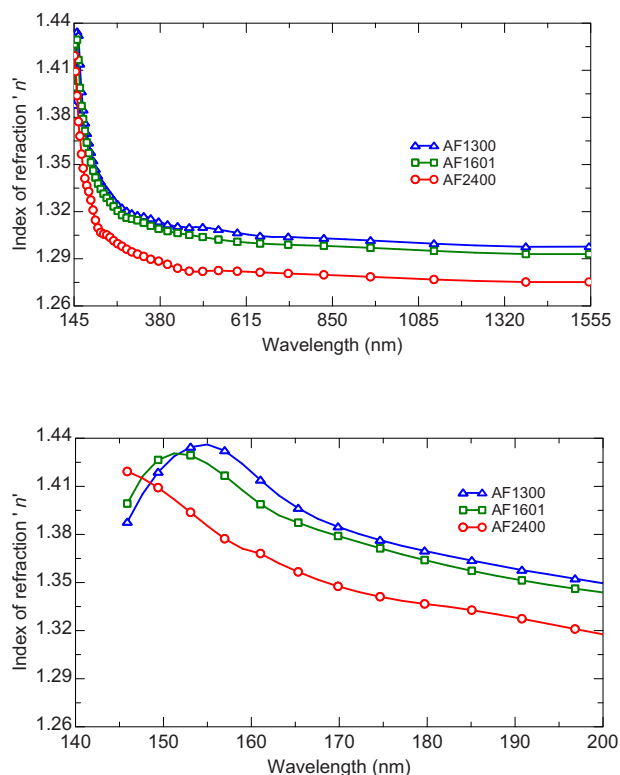


**Fig. 6** Index of refraction  $n$  determined from ellipsometric data for three grades of Teflon® AF.

The accurate measurement of transmitted light intensities is inherently difficult to attain and reproduce. The use of dual-beam spectrometers has improved accuracy and reproducibility, but the instrument relies on the equivalence of optical elements and detectors in multiple optical paths and/or the stability of the instrument over time. Since transmission-based absorbance/cm measurements result directly from the difference in transmission,  $\Delta T$ , of the substrate and the film on the substrate, the accuracy to which  $\Delta T$  can be known is a major limitation.

In addition to the variability in the measurements, the quality of the  $\text{CaF}_2$  substrates is highly variable due to bulk absorptions and surface contamination issues. These issues are more critical at 193 nm than at longer wavelengths, since materials are much more strongly absorbing at

193 nm. This variability requires that each substrate be measured before the thin film is deposited and then used in calculation of the film's absorbance/cm calculations. In more well established optical materials such as ultrahigh-purity fused silica or single-crystal sapphire, the assumption that the substrates are all comparable is an acceptable approximation. For substrates of  $\text{CaF}_2$ , transmission can vary<sup>19</sup> from 71 to 86%.

Knowledge of the film thickness is also required to determine the absorbance/cm. Determination of the thickness of a soft polymer film that is nearly index matched to a transparent substrate can be very challenging. This thickness uncertainty enters directly into the accuracy of the resulting absorbance/cm values.

The fundamental absorbance,  $A$  (base 10), and absorption coefficient,  $\alpha$  (base e), spectra versus wavelength for the three grades of Teflon® AF are shown in Figs. 4 and 5, respectively.

### 3.3 Urbach fits results

To compare with the experimental data, the Urbach edge fit to the optical absorption edge of absorbance ( $A$ ) and absorption coefficient ( $\alpha$ ) of the three grades of Teflon® AF are shown in Figs. 4 and 5. The relationship between these two ways of Urbach fitting to  $A$  or  $\alpha$  was described in Secs. 2.5.1 and 2.5.2. The Urbach edge fits underneath the measured absorption edge for energies below the fundamental absorption edge, and the Urbach edge positions are presented in Table 4 for the three grades. Typically, we found that the standard deviation of the Urbach edge position is  $\sim 1.6$  nm and of the Urbach edge width is  $\sim 0.3$  nm. There is a correlation of the Urbach edge parameters with the range of optical absorbance of the sample and, therefore, Urbach parameters should be compared for samples over wavelength ranges exhibiting comparable ranges of optical absorbance. We can also compare the absorbance at 193 nm for the measured absorbance and the Urbach absorption edge. In this case, the broad, diffuse nature of the extrinsic absorbance allows the Urbach edge fit to distinguish the extrinsic contributions from the intrinsic contributions to the optical absorbance.

**Table 3** Indices of refraction at lithographic wavelengths.

| nm    | AF1300 |       | AF1601 |       | AF2400 |       |
|-------|--------|-------|--------|-------|--------|-------|
|       | $n$    | $k$   | $n$    | $k$   | $n$    | $k$   |
| 157.0 | 1.432  | 0.031 | 1.417  | 0.026 | 1.377  | 0.006 |
| 172.2 | 1.380  | 0.004 | 1.375  | 0.007 | 1.344  | 0.000 |
| 185.1 | 1.364  | 0.002 | 1.357  | 0.002 | 1.333  | 0.000 |
| 248.0 | 1.329  |       | 1.325  |       | 1.303  |       |

**Table 4** Urbach edge fit parameters.

| TAF Grade | Urbach Edge Position (nm) from Absorbance Fits | Urbach Edge Position (nm) from Absorbance Coefficient Fits | Urbach Edge Width (nm) from Absorbance | Urbach Edge Width (nm) from Absorbance Coefficient Fits |
|-----------|--|--|--|---|
| AF1300    | 205  | 211  | 5.9                                    | 6.0   |
| AF1601    | 199  | 204  | 5.5                                    | 5.5   |
| AF2400    | 176  | 178  | 2.8                                    | 2.8   |

## 4 Discussion

### 4.1 Complex Index of Refraction

The index values of Teflon® AF1300 presented in Table 3 show that it has a higher index of refraction than Teflon® AF1601 and Teflon® AF2400 fluoropolymers. Refractive indices at other wavelengths can be determined from the Sellmeier parameters given in Table 2. But Fig. 6 shows that the index values dropped from the wavelength of 155 nm to shorter wavelengths for both AF1300 and AF2400. Also, Teflon® AF1300 shows a higher extinction coefficient ( $k$ ) at 193.4 nm (Fig. 3) than Teflon® AF1601 and Teflon® AF2400. The index values and extinction coefficient ( $k$ ) of Teflon® AF1601 are intermediate to those of Teflon® AF1300 and Teflon® AF2400. Teflon® AF2400 has the lowest index values and extinction coefficient ( $k$ ). This is consistent with the earlier observation that the refractive index increases as the TFE content increases and the PDD content decreases.<sup>1</sup>

### 4.2 Optical Absorbance

The absorbance and absorption coefficient spectra of Teflon® AF1300 presented in Table 5 show that it is more strongly absorbing at 193.4 nm (93/cm) than Teflon® AF1601 and Teflon® AF2400 fluoropolymers. This is consistent with our earlier observations.<sup>19</sup> Increasing the TFE content in the polymer increases the average  $(CF_2-CF_2)_n$  run length in the polymer chain, and this is associated with a noticeable increase in 193.4-nm absorption. Apparently, PDD interferes with the absorptive effect of long runs of adjacent  $(CF_2)_n$  groups, presumably by breaking up the electron conjugation down the polymer chain backbone in the  $CF_2$  run segments. Looking at the structure of PDD, it can be seen that the PDD monomer unit adds two adjacent O-C-F bonds (as opposed to the F-C-F of TFE) to a polymer chain. In a chain consisting of PDD and TFE monomers, such as in Teflon® AF, the presence of uninterrupted

**Table 5** Absorbance/cm values at 193.4 nm from experiment and Urbach edge analysis.

| TAF Grade | Measured Absorbance/cm | Urbach Absorption Edge/cm |
|-----------|------------------------|---------------------------|
| AF1300    | 93                     | 7.9                       |
| AF1601    | 41                     | 2.5                       |
| AF2400    | 28                     | 0.6                       |

sequences of F-C-F units down the chain is bad for absorption, while the introduction of the PDD disrupts these TFE runs and reduces their length, thereby reducing the optical absorption. Nonetheless, Teflon® AF2400, which shows the lowest absorbance, has a stiff and sterically congested chain, as evidenced by its high glass transition temperature (240°C).<sup>1</sup> We assume that the absorption of  $CF_2$  units is also dependent upon rotational angle and that the PDD monomer forces conformations are unfavorable for 193.4-nm absorption.

### 4.3 Urbach Edge Analysis and Polymer Composition

We have seen that increasing TFE content increases absorption at 193.4 nm. Therefore, the Urbach optical absorption edge positions moved to longer wavelengths and the Urbach edge width became wider as the absorption increases. Teflon® AF1300 contains ~50 mol% TFE, while AF1601 and AF2400 have lower TFE contents, at ~35 mol% and ~11 mol%, respectively. Therefore, the same TFE run-length mechanism discussed earlier can be associated with the dramatic shift of the absorption edge position with the associated change in TFE/PDD ratio.

#### 4.3.1 Urbach edge position

In Urbach analysis of the absorbance ( $A$ ), Teflon® AF1300 shows the optical absorption edge at a wavelength of 205 nm and an Urbach edge width of 5.9 nm, while analysis of the absorption coefficient ( $\alpha$ ) shows a wavelength of 211 nm and an Urbach edge width of 6.0 nm. The Urbach edge width is supposed to be the same in both analyses; however, we see a 0.1-nm difference here. Both Urbach analysis parameters are greater than with the other two grades of Teflon® AF. For Teflon® AF1601, both Urbach parameters of optical absorption edge (199 nm and 204 nm) and Urbach edge width (5.5 nm) were sandwiched between Teflon® AF1300 and Teflon® AF2400. Additionally, the Urbach fits of Teflon® AF2400 show that both Urbach parameters of optical absorption edge (176 nm and 178 nm) and Urbach edge width (2.8 nm) in analyses of absorbance ( $A$ ) and absorption coefficient ( $\alpha$ ) were less than the other two grades of Teflon® AF.

#### 4.3.2 Urbach edge absorbance at 193.4 nm

We can also compare the absorbance at 193.4 nm for the measured absorbance (93/cm) and the Urbach absorption

edge (less than 10/cm) for Teflon® AF1300. For Teflon® AF1601, the Urbach fits absorbance curve shows it to have a measured absorbance of 41/cm and Urbach absorption edge less than 3/cm at 193.4 nm. The Urbach fits absorbance curve of Teflon® AF2400, shows it to have a measured absorbance of 28/cm and an Urbach absorption edge less than 1/cm at 193.4 nm (Table 5). So in these cases, the broad, diffuse nature of the extrinsic absorbers allows the Urbach edge fit to distinguish the extrinsic contributions from the intrinsic contributions to the optical absorption.

## 5 Conclusions

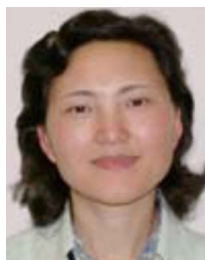
Three grades of Teflon® AF fluoropolymers have been studied using ellipsometry and transmission measurements to determine their optical properties. These three Teflon® AF grades have differing copolymer compositions (the ratio of TFE/PDD in mol%) and compositional differences that give rise to systematic changes in the optical properties such as the index of refraction and absorption coefficient. A comparison of the absorbance at 193.4 nm and the Urbach fit absorption edge of the three grades of Teflon® AF fluoropolymers suggests that extrinsic absorbers may account for a small increase in absorbance over what might be the intrinsic absorbance of the polymer. We found that the optical properties of the three grades of Teflon® AF varied systematically with the AF TFE/PDD composition. The indices of refraction, extinction coefficient ( $k$ ), absorption coefficient ( $\alpha$ ), and absorbance ( $A$ ) increased, as did the TFE content, while the PDD content decreased. In addition, the Urbach edge position moved to a longer wavelength, and the Urbach edge width became wider.

## Acknowledgments

The authors acknowledge the assistance of Dr. Lin K. DeNoyer (Spectrum Square Associates, Inc.) for Urbach analysis programming and Sellmeier parameters determination, B. B. French for editing the manuscript, and Mike Lemon, Bob Balback, and Mike Reilly for assistance in the measurements.

## References

1. P. R. Resnick and W. H. Buck, in *Modern Fluoropolymers*, J. Schiers, Ed., pp. 397–419, Wiley, West Sussex, England (1997).
2. G. Belanger, P. Sauvageau, and C. Sandorfy, "The far-ultraviolet spectra of perfluoro-normal-paraffins," *Chem. Phys. Lett.* **3**(8), 649 (1969).
3. K. Seki, H. Tanaka, T. Ohta, Y. Aoki, A. Imamura, H. Fujimoto, H. Yamamoto, and H. Inokuchi, "Electronic structure of poly(tetrafluoroethylene) studied by UPS, VUV absorption, and band calculations," *Phys. Scr.* **41**, 167 (1990).
4. T. M. Bloomstein, M. Rothschild, R. R. Kunz, D. E. Hardy, R. B. Goodman, and S. T. Palmacci, "Critical issues in 157 nm lithography," *J. Vac. Sci. Technol. B* **16**(6), 3154 (1998).
5. B. Johs, R. H. French, F. D. Kalk, W. A. McGahan, J. A. Woollam, "Optical interference coatings," *Proc. SPIE* **2253**, 1098 (1994).
6. J. A. Woollam, B. Johs, C. M. Herzinger, J. Hilfiker, R. Synowicki, C. L. Bungay, "Overview of variable angle spectroscopic ellipsometry (VASE), part I: basic theory and typical applications," *Proc. SPIE* **CR72**, 3–28 (1999).
7. R. H. French, J. S. Meth, J. R. G. Thorne, R. M. Hochstrasser, and R. D. Miller, "Vacuum ultraviolet spectroscopy of the optical properties and electronic structure of seven poly(di-alkylsilanes)," *Synth. Met.* **50**(1–3), 499–508 (1992).
8. M. E. Innocenzi, R. T. Swimm, M. Bass, R. H. French, and M. R. Kokta, "Optical absorption in undoped yttrium aluminum garnet," *J. Appl. Phys.* **68**(3), 1200–1204 (1990).
9. M. E. Innocenzi, R. T. Swimm, M. Bass, R. H. French, A. B. Villaverde, and M. R. Kokta, "Room temperature optical absorption in undoped  $\alpha$ -Al<sub>2</sub>O<sub>3</sub>," *J. Appl. Phys.* **67**(12), 7542–7546 (1990).
10. J. A. Woollam, B. Johs, C. M. Herzinger, J. Hilfiker, R. Synowicki, and C. L. Bungay, "Overview of variable angle spectroscopic ellipsometry (VASE), part II: advanced applications," *Proc. SPIE* **CR72**, 29–58 (1999).
11. B. Johs, R. H. French, F. D. Kalk, W. A. McGahan, and J. A. Woollam, "Optical analysis of complex multilayer structures using multiple data types," in *Optical Interference Coatings*, F. Abeles, Ed., *Proc. SPIE* **2253**, 1098–1106 (1994).
12. F. Wooten, *Optical Properties of Solids*, p. 49, Academic Press, New York (1972).
13. W. Sellmeier, "II. Regarding the sympathetic oscillations excited in particles by oscillations of the ether and their feedback to the latter, particularly as a means of explaining dispersion and its anomalies," [in German], *Ann. Phys. Chem.* **147**, 524–54 (1872); [http://en.wikipedia.org/wiki/Sellmeier\\_equation](http://en.wikipedia.org/wiki/Sellmeier_equation).
14. R. H. French, R. C. Wheland, D. J. Jones, J. N. Hilfiker, R. A. Synowicki, F. C. Zumsteg, J. Feldman, and A. E. Feiring, "Fluoropolymers for 157-nm lithography: optical properties from VUV absorbance and ellipsometry measurements," in *Optical Microlithography XIII*, C. J. Proglor, Ed., *Proc. SPIE* **4000**, 1491–1502 (2000).
15. R. H. French, J. Gordon, D. J. Jones, M. F. Lemon, R. C. Wheland, E. Zhang, F. C. Zumsteg, K. G. Sharp, and W. Qiu, "Materials design and development of fluoropolymers for use as pellicles in 157-nm photolithography," in *Optical Microlithography XIV*, C. J. Proglor, Ed., *Proc. SPIE* **4346**, 89–97 (2001).
16. R. H. French, K. I. Winey, M. K. Yang, and W. Qiu, "Optical properties and van der Waals-London dispersion interactions of polystyrene determined by vacuum ultraviolet spectroscopy and spectroscopic ellipsometry," *Aust. J. Chem.* **60**, 251–263 (2007).
17. R. H. French, H. Sewell, M. K. Yang, S. Peng, D. McCafferty, W. Qiu, R. C. Wheland, M. F. Lemon, L. Markoya, and M. K. Crawford, "Imaging Of 32-nm 1:1 lines and spaces using 193-nm immersion interference lithography with second-generation immersion fluids to achieve a numerical aperture of 1.5 and a k1 of 0.25," *J. Microolithogr., Microfabr., Microsyst.* **4**(3), 031103 (2005).
18. F. Urbach, "The long-wavelength edge of photographic sensitivity and of the electronic absorption of solids," *Phys. Rev.* **92**, 1324 (1953).
19. R. H. French, R. C. Wheland, W. Qiu, M. F. Lemon, E. Zhang, J. Gordon, V. A. Petrov, V. F. Cherkstkov, and N. I. Delayagina, "Novel hydrofluorocarbon polymers for use as pellicles in 157-nm semiconductor photolithography," *J. Fluorine Chem.* **122**, 63–80 (2003).



**Min K. Yang** is a staff technologist in Central Research at the DuPont Company in Wilmington, Delaware. She received her master's degree in materials science and engineering from Virginia Tech in 1994. She joined DuPont in 2000 and has been involved in several projects. Currently, she works on immersion lithography, where she focuses on optical properties characterization for immersion fluids. She has contributed to several papers and patents in the area of immersion lithography.



**Roger H. French** holds a PhD in materials science from MIT, where his work involved vacuum ultraviolet spectroscopy on Al<sub>2</sub>O<sub>3</sub> from 80 to 800 nm. He is a research fellow in materials science in Central Research at the DuPont Company in Wilmington, Delaware, and also an adjunct professor of materials science at the University of Pennsylvania. His research is in optical properties and the electronic structure of ceramics, optical materials, and polymers. His work on new materials for optical lithography for integrated circuit fabrication has produced attenuating phase shift photomasks, photomask pellicles, semiconductor photoresists, and most recently, lithographic immersion fluids. He also works on the origins and applications of London dispersion forces and the electronic structure and wetting of interfaces, such as intergranular and surficial films. He studies near-field optics and scattering by particulate dispersions and complex microstructures using computational solutions to Maxwell's equations. His work has produced 17 issued patents 135 published papers.





**Edward W. Tokarsky** received a BS in ceramic science and technology from Penn State University and a PhD in materials engineering from Rensselaer Polytechnic Institute, with thesis work on carbon fiber funded by the US Air Force. After graduate school, he joined Hercules, Inc., where he developed advanced carbon fibers for a wide variety of applications including carbon-carbon composites, thermosetting acetylenic polymers, and high-toughness propylene copolymer systems. Moving to DuPont-Advanced Fibers Systems in 1979, he made significant contributions to new business

developments for Kevlar and Nomex in structural aircraft composites, printed circuit board reinforcements, and advanced honeycomb materials. He led the Aracon metal-clad aramid fibers team in developing lightweight, high-strength electromagnetic shielding and signal conductors, with key adoptions in the U-2 fleet and JSF. He joined Fluoropolymer Solutions in 2001 as a technical consultant supporting developments of fluoropolymer wire insulation systems in aircraft/aerospace. His current responsibilities involve technical service and growth initiatives for amorphous fluoropolymers in a wide range of applications. He is the author of numerous technical publications related to the various business developments over the years, has over 12 patents.